Please cite this article as:
Banks, L.K., Lavoie, I., Robinson, C.E., Roy, J.W., and Yates, A.G. 2023. Effects of groundwater inputs on algal assemblages and cellulose decomposition differ based on habitat type in an agricultural stream. *Hydrobiologia*. https://doi.org/10.1007/s10750-023-05251-1

Effects of groundwater inputs on algal assemblages and cellulose decomposition differ based on habitat type in an agricultural stream

LK Banks[1*], I Lavoie[2], CE Robinson[3], JW Roy[3,4], and AG Yates[1]

1. **Department of Biology, University of Waterloo, Waterloo ON, Canada**
   Lauren K Banks ORCID: 0000-0001-6197-4245, Adam G Yates ORCID: 0000-0002-2239-9046
2. **Institut national de la recherche scientifique, centre Eau Terre Environnement, Québec, QC, G1K 9A9, Canada**
   Isabelle Lavoie ORCID: 0000-0002-2918-6297
3. **Department of Civil and Environmental Engineering, Western University, London ON, N6A 5B9, Canada**
   Clare E Robinson ORCID: 0000-0002-6156-2328
4. **Water Science and Technology Directorate, Environment and Climate Change Canada, Burlington ON, Canada, L7S 1A1**
   James W Roy ORCID: 0000-0002-1804-2917
   *Corresponding author e-mail: laurenkbnks@gmail.com

Acknowledgments

This work was supported by grants provided to CE Robinson and AG Yates via a Natural Sciences and Engineering Research Council of Canada Strategic Project Grant (STPG 506523) and an Ontario Graduate Scholarship (2019) and NSERC Postgraduate Scholarship (2020) to LK Banks. We would like to thank the members of the StrEAMS lab and RESTORE lab for laboratory and field assistance, especially Erika Hill, Amy White, Cora Bilhorn, Meghan Vissers, Shuyang Wang, and Kyle Robinson. We thank two anonymous reviewers for their comments on earlier drafts of this manuscript.

Abstract

Stream communities and processes are known to differ among reaches and habitat types in accordance with environmental variation. However, groundwater input has not been well-explored as a driver of ecological heterogeneity among stream reaches and habitats. We assessed stream biofilm communities (biomass and diatom assemblage composition) and cellulose decomposition in run and riffle habitats across three stream reaches with high, moderate, and low groundwater input in Kintore Creek, Ontario, Canada. Algal biomass, as well as density and composition of diatom assemblages, differed between runs and riffles in reaches with moderate and high groundwater inputs, but not in the low groundwater reach. Reaches with moderate and high groundwater input had faster streambed cellulose decomposition in riffles than in runs, whereas the reach with low groundwater input had no difference in streambed cellulose decomposition. Subsurface cellulose decomposition in riffles and runs was fastest in the high groundwater reach. We found that measured environmental variables did not explain the apparent effects of groundwater inputs. Findings from this study highlight the covarying influence of groundwater input and habitat type in altering in-stream ecological response in enriched streams.

Keywords: Diatoms, Chlorophyll-*a*, Biomass, Cellulose Decomposition, Radon, Habitat, Riffle, Run, Ecological heterogeneity

Introduction

Stream biofilms are an essential component of stream ecosystem structure and function because of their role in biogeochemical processing of organic and inorganic materials (Borchardt, 1996; Battin et al., 2003; Besemer, 2015). Stream biofilms are composed of autotrophic and heterotrophic microorganisms that include algae, bacteria, and fungi (Besemer, 2015). The algal component of biofilms influences nutrient cycling in streams through uptake and subsequent transformation and/or remineralization of nutrients, and generates primary production that is a source of basal resources for higher trophic levels (Minshall, 1978; Borchardt, 1996; Mulholland, 1996). Likewise, heterotrophic microorganisms in the biofilm contribute to carbon cycling in streams through conversion of organic material into smaller particles, as well as mineralization and assimilation into microbial biomass (Cummins, 1974; Petersen & Cummins, 1974). Due to the critical functions biofilms perform in streams, considerable effort has been made to identify environmental factors that influence biofilm communities (e.g., biomass and diatom assemblage composition) and organic matter breakdown (e.g., in Biggs, 1995; Biggs et al., 1998; Lavoie et al., 2014; Battin et al., 2016; Tiegs et al., 2019).

Environmental factors that have been found to be important determinants of stream biofilm communities and organic matter breakdown include light, nutrients, water temperature, water chemistry, and stream velocity (Stevenson, 1997; Royer & Minshall, 2003; Graça et al., 2015). Further, these environmental factors act on biofilm communities and organic matter breakdown at different spatial scales. For example, previous work has shown that surface water nutrients, water temperature, and water chemistry can vary at the reach scale (Biggs, 1995; Stevenson, 1997; Martínez et al., 2014; Graça et al., 2015). Stream velocity is a key environmental factor that varies at the habitat scale (Biggs et al., 1998, 2005; Passy, 2007; Webb et al., 2019). Surface water nutrient availability, water temperature, and water chemistry can also be influenced by groundwater inputs at reach and habitat scales (Boulton & Hancock, 2006; Boano et al., 2014). However, the extent that habitat type may modify the effect of groundwater inputs and subsequently alter patterns in stream biofilm communities and organic matter breakdown has not been well-studied.

In streams, groundwater inputs are often spatially heterogeneous due to varying hydraulic gradients between groundwater and surface waters, as well as subsurface hydrogeological

structures that result in variable groundwater flow paths (Conant et al., 2019). Within reaches, groundwater flow paths can be modified by hydrogeomorphic features including sequences of faster stream velocity (i.e., riffle habitats) to slower stream velocity (i.e., run habitats), with changing stream velocities and streambed topography resulting in patchiness in groundwater inputs due to differences in hydraulic head (Harvey & Bencala, 1993; Brunke & Gonser, 1997). Additionally, heterogeneity in streambed permeability can affect the connectivity patterns in groundwater – surface water exchange. For example, coarse sediment typically allows for greater exchange, whereas finer sediment inhibits exchange (Renard & Allard, 2013). Groundwater inputs can modify a stream's environmental conditions when the surface water and groundwater have different physical and chemical characteristics. For example, depending on season, upwelling groundwater can have lower (summer) or higher (winter) water temperature than surface waters (Krause et al., 2011). Alternatively, groundwater can be more reducing compared to surface waters leading to redox gradients near the groundwater – surface water interface that can affect the release and retention of nutrients (Lewandowski et al., 2019; Vissers et al., 2023).

Changes in environmental conditions due to spatially heterogeneous groundwater inputs have been linked to patterns in stream biofilm communities and cellulose decomposition. At the reach and habitat scales, input of groundwater has been associated with elevated primary production (Coleman & Dahm, 1990; Roy et al., 2011; Mejia et al., 2016; Burrows et al., 2020). Further, past work has suggested that groundwater inputs can stimulate cellulose decomposition by providing nutrient subsidies (Griffiths & Tiegs, 2016), but may also reduce cellulose decomposition through stream cooling (Webb et al., 2019, Poisson & Yates, 2022). Additionally, lower dissolved oxygen in groundwater inputs may also lead to slower decomposition rates (Cornut et al., 2010). However, there has been limited work explicitly assessing how the impact of groundwater inputs on stream environmental conditions, biota, and processes may differ among habitats (but see Burrows et al., 2020).

Within a reach, habitat type can generate environmental heterogeneity that could modify the impact of groundwater inputs and associated patterns in stream biofilm communities and cellulose decomposition (Webb et al., 2019; Burrows et al., 2020). Habitat type is often defined by relative stream velocity, where fast moving water is associated with riffles and slower moving water is associated with runs and/or pools (Jowett, 1993). Differences in stream velocity have been shown to alter biofilm communities and organic matter processing. For example, faster

stream velocity produces increased shear stress, which is an important driver in determining which taxa establish in algal assemblages (Biggs & Hickey, 1994; Biggs et al., 1998). Rates of organic matter processing are also enhanced by faster stream velocity due to greater physical abrasion (Clapcott & Barmuta, 2010). Further, physical differences between habitat types have been associated with spatial heterogeneity in groundwater input. In riffles, a sudden steepening of the slope of the streambed results in faster stream velocities, but can also create a pressure differential at the streambed surface along the riffle driving surface water to downwell at the start of riffles and upwell at the end of the riffle (i.e., a hyporheic flow path) (Harvey & Bencala, 1993). This hyporheic flow across the riffle can result in groundwater inputs being restricted to the end of the riffle or beginning of the adjacent run, and to the edges of the stream. In contrast, for a run, the streambed topography and slope are more muted, resulting in lower stream velocities and limited pressure differentials, and thus limited hyporheic flow to restrict groundwater inputs (Dent et al., 2001).

Our study compared stream biofilm communities and cellulose decomposition in riffle and run habitats in reaches with high, moderate, and low groundwater inputs and determined if impacts of groundwater input were habitat dependent. We also assessed if environmental variables modified by groundwater inputs were associated with habitat scale patterns in biofilm communities and cellulose decomposition. We hypothesized that differences in groundwater inputs and subsequent changes in environmental conditions would result in heterogeneity in biofilm biomass and composition and cellulose breakdown among reaches with varying groundwater inputs. Our results provide insight into the role of groundwater inputs as a driver of biofilm communities and cellulose decomposition, and how habitat type may constrain the impacts of groundwater inputs.

Methods

Study area and site selection

Our study used a hierarchical design to assess the role of groundwater in generating environmental variation at reach and habitat scales, and if that variation is a driver of ecological heterogeneity in stream biofilm communities (biomass and diatom assemblage) and cellulose decomposition. This study was conducted in three headwater reaches in Kintore Creek, southern Ontario, Canada (Fig. 1a, b). Kintore Creek experiences a temperate climate, with mean annual

low and high air temperatures of -6.0 °C and 20.2 °C, respectively, and average annual precipitation of 1069.5 mm (Environment and Climate Change Canada, 2010). Land use in the Kintore Creek catchment is predominantly agricultural (80 %), with forest (12 %) and residential (4 %) uses comprising smaller portions (Agricutlure and Agri-Food Canada, 2020). Crop cover in the catchment consists of soybean, corn, and alfalfa, and many fields are tile drained. Surficial geology in the catchment varies in permeability in association with glacial deposits of tills (low permeability) to sands and gravels (high permeability) (Ontario Geological Survey, 2010).

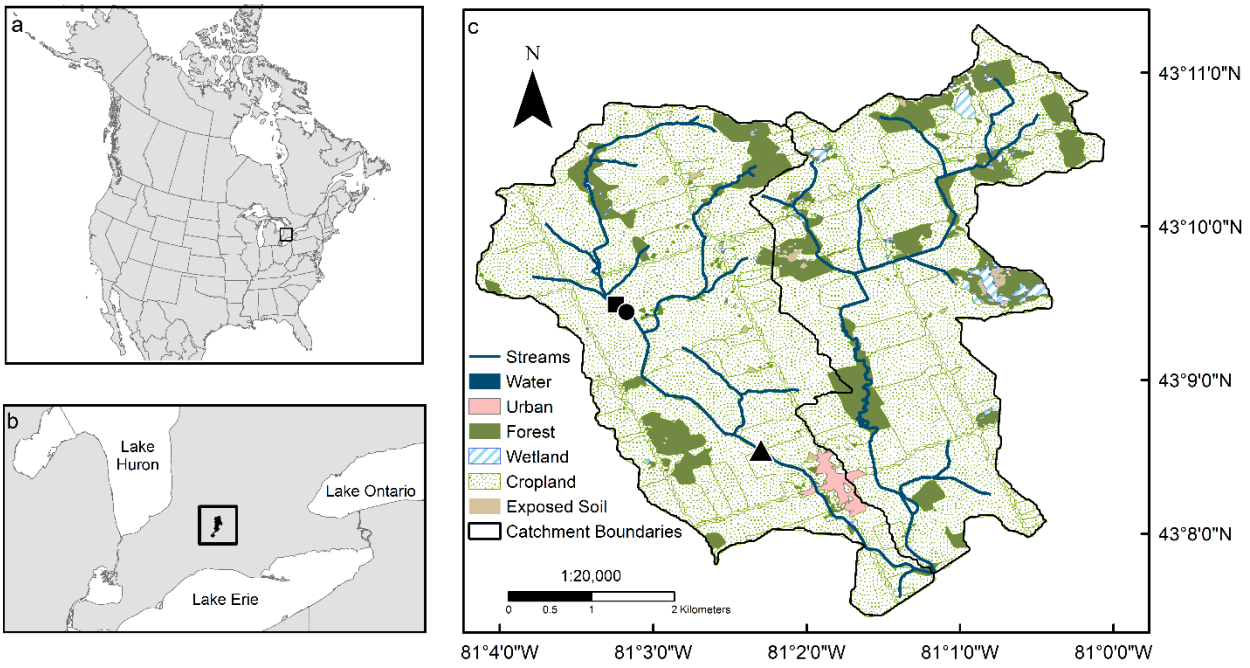

Fig. 1 Locations of study area in North America (a) and the Kintore creek catchment in southern Ontario (b). Placement of high (HG; filled triangle), moderate (MG; filled square), and low (LG; filled circle) groundwater reaches in western headwater branch of the agriculturally dominated Kintore Creek catchment are indicated in panel c. (Catchment boundaries/stream network in Forsyth et al., 2016; Land use/cover in Agricutlure and Agri-Food Canada, 2020)

Reaches assessed in this study were selected based on differences in groundwater input identified using radon-222 (^{222}Rn, Bq m^{-3}). ^{222}Rn is widely used as a tracer for identifying groundwater inputs as ^{222}Rn concentrations are typically orders of magnitude higher in groundwaters compared to receiving surface waters, where it undergoes gas evasion and decay (Cook, 2013). A single surface water sample was collected above and below each reach using 4 L

amber glass bottles and analyzed for ^{222}Rn less than 4 hours after collection using RAD7 electronic radon detectors with the big bottle accessory (Durridge, USA).

A steady state ^{222}Rn mass balance model was then used to estimate net groundwater discharge across each stream reach based on the in-stream ^{222}Rn concentrations (Table 1). The model is based on Atkinson et al. (2015) and considers ^{222}Rn inputs to the stream from groundwater and ^{222}Rn losses due to gas evasion (Supplemental Information 1). The mass balance model results were used to identify three reaches with varying groundwater inputs: 1) high groundwater reach (hereafter HG); 2) moderate groundwater reach (hereafter MG), and; 3) low groundwater reach (hereafter LG) (Fig. 1c). HG is approximately 45 m in length, whereas MG and LG were about 50 m in length. LG is approximately 20 m downstream from MG.

Stream water chemistry and nutrient conditions were measured in each reach. Soluble reactive phosphorus (SRP) and nitrate – nitrogen (NO_3-N) were measured at three locations in each reach (top, middle, end) three times (beginning, middle, end) during the experiment. SRP was analyzed using a Flow Injection Analysis automated ion analyzer (FIA) (Lachat QuikChem, QC8500 FIA Automated Ion Analyzer, LDL 1 μg L^{-1}). NO_3^--N was analyzed using liquid chromatography (HPLC) (Thermo Scientific Dionex Aquion Ion Chromatography System with Dionex AS-DV autosampler, LDL 0.25 mg L^{-1}). pH and specific conductivity were measured at 5 locations in each habitat mid-way through the experiment using a handheld YSI probe (YSI, Professional Plus). Aside from differences in the groundwater inputs, the three selected reaches showed little variability among most environmental conditions with the exception of channel substrate. HG substrate was generally gravel and sand, substrate in MG was primarily cobble and gravel, whereas at LG the streambed was primarily finer sediment (clay and fine sand). All reaches had open canopies, with surface water nutrients, pH, and specific conductivities (μS cm^{-1}) comparable among the reaches during the deployment period (Table 1).

Table 1 ^{222}Rn and mean ± standard deviation of stream water chemistry and nutrient conditions in study reaches during deployment. ^{222}Rn Above and ^{222}Rn Below indicate ^{222}Rn concentration above the reach and below the reach, respectively. Groundwater discharge is for entire reach and was calculated using the ^{222}Rn mass balance model.

Environmental Parameter	**HG**	**MG**	**LG**
Radon			

^{222}Rn Above (Bq m^{-3})	1183	295	679
^{222}Rn Below (Bq m^{-3})	1121	679	782
Groundwater discharge (m^3 d^{-1} m^{-1})	7.1	2.7	1.0
Water Chemistry			
SRP (µg P L^{-1})	25.5 ± 3.0	37.6 ± 3.5	38.4 ± 4.7
NO_3-N (mg N L^{-1})	4.9 ± 0.6	3.4 ± 1.0	3.3 ± 1.2
pH	8.07 ± 0.01	8.02 ± 0.01	8.02 ± 0.01
Sp. conductivity (µS cm^{-1})	644 ± 1.6	644.1 ± 0.9	642.5 ± 0.5

Sample Collection & Processing

This study was conducted from July 3rd to August 6th in 2019. Within each reach, sampling locations were established in two riffles and two runs. Riffles and runs were distinguished based on differences in stream velocity (m/s) and depth (cm). Within each habitat unit, five locations in the middle of the channel along the length of the habitat unit were selected for assessment of algal biofilms and cellulose decomposition.

Algal biofilms

To provide a consistent surface for stream biofilm accumulation, we sampled biofilms using standardized artificial substrates (unglazed ceramic tiles; 21.24 cm^2 each, *sensu* Steinman et al., 2007). Three tiles were inserted into a tile holder, then the tile holder was affixed to a brick anchor using cable binders. To secure the tile holder and its brick anchor, the brick was buried in the streambed while ensuring the tile holder 'lip' was placed approximately 2 cm above the streambed. Tile holders were placed at each of the five positions within each habitat unit and were incubated for 26 or 27 days. For each position, two tiles were sampled for biomass (one tile each for chlorophyll-*a* [chl-*a*] and ash-free dry mass [AFDM]) by scraping all biofilm material from entire tile surface using a toothbrush. Because diatoms have shown strong responses to changes in water quality (e.g. nutrients, pH, salinity) (Lavoie et al., 2014), we sampled the third tile for diatom assemblages. Samples for diatom analysis were preserved with Lugol's iodine (~1% v/v), and biomass samples were placed on ice and stored frozen until chl-*a* and AFDM analyses.

Diatom samples were prepared for enumeration by acid digestion in 5 mL of 100% (v/v) nitric acid for 15 h to remove organic matter, ensuring visible diatom frustules. To complete

digestion, 1 mL of hydrogen peroxide 30 % (v/v) was added to each sample, then tubes were immersed in a hot water bath at 60 °C for 1 h. Once cooled to room temperature, samples were centrifuged for 10 minutes at 5500 rpm and the acid supernatant was discarded and pellets retained. Deionized water was added to rinse pellets and this step was repeated until the supernatant was above a pH of 6. Naphrax® (refractive index: 1.74; Brunel microscopes Ltd., Wiltshire, UK) was used to mount diatom frustules on microscope slides. Lastly, diatom assemblages were enumerated at a 1000x magnification using an Olympus BX51 Upright Compound Microscope equipped with differential interference contrast optical components. A minimum of 400 diatom valves per sample were enumerated and identified to species level, where possible, following Lavoie et al. (2008) and Bey & Ector (2013).

Frozen chl-*a* samples were thawed and then filtered onto Whatman GF/C filters. Filters were submerged in 10 mL of 90% ethanol in 50 mL centrifuge tubes. A hot ethanol, non-acidification extraction was done by inserting centrifuge tubes into an 80 °C hot water bath for 7 min. The chl-*a* concentration for each sample was determined using a Turner Designs Trilogy Fluorometer (Model: 7200e000). If maximum detection limits (> 75 µg/mL) were exceeded, then extracted liquid was diluted. We calculated chl-*a* accumulation by dividing chl-*a* concentration by number of days incubated in the stream to standardize samples.

Frozen AFDM samples were thawed prior to analysis. Upon analysis, samples were filtered through pre-ashed Whatman GF/C filters and dried at 105 °C for at least 12 h. For determination of organic mass, the filtered and dried samples were then weighed. Samples were then ashed in a muffle furnace at 550 °C for 1 h. After cooling to room temperature, ashed filters were weighed to determine mass loss on ignition. Because of high levels of silt/clay in the samples, samples were then re-wetted and dried for a minimum of 12 h at 105 °C. The samples were then weighed to correct for water loss due to the presence of clay and other minerals. To standardize samples, we calculated biofilm growth rate by dividing AFDM by number of days incubated in the stream.

Cellulose Decomposition

We used the cotton strip assay (CSA; Tiegs et al., 2013) to measure cellulose decomposition. Cotton strip preparation, deployment, and retrieval followed Tiegs et al. (2013). Cotton strips were made using Fredrix-brand unprimed 12-oz. heavyweight cotton fabric, Style

#548 (Fredrix, Lawrenceville, GA, USA) by producing 2.5 cm x 8 cm strips, with 3 mm of frayed 'fuzz' on the length of the fabric strip.

Ten cotton strips were randomly assigned to each position. Five cotton strips were attached to the tile holder using cable binders, so they laid flat on the surface of the streambed. The remaining five strips were buried at 10 cm depth in the streambed sediment. Both surface and subsurface cotton strips were incubated for 14 days.

Immediately after retrieval, strips were immersed in a tray containing 70 % ethanol for 7 minutes to sterilize the strip, halting microbial activity. Once sterilized, strips were carefully brushed to remove excess debris and sediment. Sterilized and cleaned strips were laid flat and fully covered in folded aluminum foil, then placed on ice in a cooler until we returned to the lab. Strips were then dried at 40 °C for 24 h in the lab, which was then followed by evaluation of tensile strength.

Tensile strength, defined here as the force required to break the strip, was measured for each strip using a tensiometer and motorized test stand (Force Gauge, Model M3-100). Using methods outlined by Tiegs et al. (2013), equal lengths of the strip were positioned in the tensiometer grips (Mark-10 brand, Model #MG100). Next, strips were pulled at a constant rate of 2 cm/min until peak tension, identified as when the strip ripped, was reached. To determine percent loss of tensile strength, mean tensile strength of reference strips were compared to measured tensile strength of incubated strips. To ensure comparability between reference and stream incubated sample strips, reference strips were deployed in a mock field experiment. In the lab, reference strips were saturated in distilled water, then immersed in 70 % ethanol for 7 minutes and gently brushed. Reference strips were dried at 40 °C for 24 h, and the tensile strength of the reference strip was measured. Tensile strength was measured for each sample strip, which was then used to calculate percent tensile loss per day using Eq.1 (*sensu* Tiegs et al., 2013).

$$\%\ \text{tensile loss per day} = \frac{\left(\frac{\text{Tensile Strength}^{REF} - \text{Tensile Strength}^{SAMP}}{\text{Tensile Strength}^{REF}}\right) \text{x } 100}{\text{Incubation time}} \quad \text{(Eq. 1)}$$

Environmental characterization

Surface water temperature and stream velocity was measured in each habitat unit. Near-streambed water temperature was measured at 10-minute intervals using temperature loggers (HOBO Pendant, Onset, USA) that were anchored at the streambed surface in the center of each habitat unit for the duration of the deployment period. However, the loss of the temperature logger in one riffle in HG resulted in the loss of temperature data for that habitat unit. Mean daily temperature range (°C) and mean daily temperature (°C) were calculated from near-streambed water temperature measurements during the deployment period. Mean daily temperature range was calculated by computing daily maximum and minimum temperatures for each deployment day, then these values were averaged over the incubation period. Mean daily temperature was calculated as the sum of the daily mean temperature divided by days in the deployment period (*sensu* Benfield et al., 2017). At each tile holder, stream velocity (m/s) (Hach FH950 Portable Velocity Meter, Hach Ultra Analytics) was measured at the streambed.

Streambed temperature mapping was conducted on July 5th, 2019 in HG and on July 16th, 2019 in MG and LG. Streambed temperature can be used as a proxy for groundwater flux with temperature differences between subsurface streambed temperature and stream surface water temperature able to identify areas of groundwater input (Kalbus et al., 2006). Typically, larger temperature gradients (i.e., near-streambed surface water temperature – subsurface streambed temperature) indicates greater groundwater input. For the streambed temperature mapping, streambed temperature readings were taken at 0.3 m intervals across the stream width, with measurement transects every 1 m along the reach. Subsurface streambed temperature was measured at 10 cm depth below the streambed using a high-accuracy thermometer (Hanna HI98509 Checktemp® 1 Digital Thermometer). For each transect, near-streambed surface water temperature was measured once in the centre of the stream.

Data Analysis

We used generalized linear models (GLMs) to detect effects of groundwater input and habitat on biofilm biomass (i.e., chl-*a* accumulation and biofilm growth rate). We also applied GLMs to assess four diatom assemblage metrics: taxa richness, proportion of the three most abundant taxa (% dominant), taxa evenness, and density of diatoms. Density of diatoms was estimated by correcting the diatom counts in accordance with the proportion of the sample processed to reach 400 valves. The processed sample proportion was measured by the volume of

sample used to produce the slides and the number of fields of view necessary to reach the target count of 400 valves.

For all models, fixed effects were groundwater input (three levels: HG, MG, and LG) and habitat (two levels: riffle and run) and their interaction (groundwater input x habitat). Separate GLMs were used to test for differences ($\alpha = 0.10$) in biomass and diatom assemblage metrics. Tukey's post-hoc tests were performed on significant GLM analyses to identify pairwise differences between factor levels. We used $\alpha = 0.10$ for our GLMs to offset risk of Type I and Type II errors due to the combined effects of small sample size ($n = 10$ per habitat type) and inherent variation of biofilm biomass and diatom assemblage metrics in streams. Analyses were completed in R (version 4.0.5) using the *stats* package (R Core Team, 2020) and taxa evenness was calculated using the *vegan* package (Oksanen et al., 2020).

Linear mixed effects models (LMEMs) were used for analyses of streambed and subsurface % tensile loss per day due to the nested structure of our data. For LMEMs, strip position nested within habitat and reach was set as a random effect. Fixed effects were the same as for the GLMs used to analyze the biofilm metrics. Significant LMEM analyses were then further investigated using GLMs to identify patterns in groundwater input, habitat, and their interaction. LMEMs were computed in R (version 4.0.5) with *lme4* and *lmerTest* packages (Bates et al., 2015; Kuznetsova et al., 2017), using Satterhwaite's method to estimate degrees of freedom and p-value for fixed effects. GLMs were processed in R (version 4.0.5) using the *stats* package (R Core Team, 2020).

Spatial patterns in diatom assemblage composition among groundwater input and habitat units was assessed using non-metric multidimensional scaling (nMDS) on relative abundance data. Relative abundance data included taxa that accounted for at least 2 % relative abundance in at least one sample in any reach, and was subsequently Hellinger transformed (Legendre & Gallagher, 2001). A two-dimensional nMDS was performed using Bray-Curtis distance with a maximum of 1000 iterations or until two convergent solutions were found. Analyses were completed with PRIMER software package (version 7.0 with PERMANOVA+, Primer-E Ltd., Plymouth, UK; Clarke & Gorley, 2015).

A two factor permutational analysis of variance (PERMANOVA) was performed to compare variation in diatom assemblage composition in response to the fixed factors of groundwater input (HG, MG, and LG) and habitat unit (run, riffle). If diatom assemblage

composition in reach or habitat or their interaction were identified as significantly different (α = 0.10), we then used similarity percentages (SIMPER) routine to identify taxa which contributed most to dissimilarity among reaches and habitats. Analyses were conducted with PRIMER software package (version 7.0 with PERMANOVA+, Primer-E Ltd., Plymouth, UK; Clarke & Gorley, 2015).

To evaluate the association of environmental conditions (i.e., mean daily temperature range [°C], mean daily temperature [°C], tile depth [cm], and stream velocity [m/s]) with spatial patterns in biofilm biomass (chl-*a* accumulation and biofilm growth rate) and cellulose decomposition we used partial least squares (PLS) regression. Separate PLS analyses were conducted for biofilm biomass and % tensile loss per day on the streambed surface. PLS regression can be used to identify associations between predictor (environment) and response (ecological) variables, and is a useful tool when predictors are highly correlated, and there are many predictors relative to observations (Wold et al., 2001; Carrascal et al., 2009). For both % tensile loss per day on the streambed surface and biofilm biomass environmental predictor variables (X: mean daily temperature range [°C], mean daily temperature [°C], tile depth [cm], and stream velocity [m/s]) were used to produce a set of components (PLS loadings) that maximize variance explained for % tensile loss per day and biofilm biomass (chl-*a* accumulation and biofilm growth rate) (Y), constructed using simultaneous decomposition of X and Y matrices (Eriksson et al., 2013). Cross-validated goodness of prediction (Q^2) was used to assess model performance, where goodness of prediction ($Q^2 > 0.097$) is computed as the difference between predicted and observed values using a tenfold cross-validation method with 999 iterations. The total explanatory capacity of the PLS model is defined as the sum of explanatory capacity (R^2 Y) for each component, and only components that account for 10 % or more of the variation in response (Y) variables were retained. Variable importance projection (VIP) scores were used to assess the influence of each predictor (X) variable, and only predictors with a VIP score greater than one were considered important for explaining response (Y) variables. Using a biplot, the direction of association between predictor and response variables was assessed using resultant loadings. PLS analyses were done in R (version 4.0.3) using the *plsdepot* package (Sanchez, 2016).

We used a BIOENV (matching of biotic and environmental patterns; Clarke & Warwick, 1994) to evaluate associations between measured environmental variables (mean daily temperature range [°C], mean daily temperature [°C], tile depth [cm], and stream velocity [m/s], pH, specific

conductivity [µS/cm]) and diatom assemblage composition. Using a Spearman rank correlation, the BIOENV computes the extent of the association between two (dis)similarity matrices, resulting in pairs of samples where similar environmental variables are associated with similar diatom assemblage composition (Clarke & Warwick, 1994). To create the biotic matrices for the diatom assemblage composition we used Bray-Curtis distance on Hellinger transformed relative abundance data for taxa that comprised at least 2 % of relative abundance in a minimum of one sample in a given reach. Environmental matrices were constructed using Euclidean distance on normalized environmental variables (Clarke & Warwick, 1994). Analyses were conducted with *bioenv* function and significance was tested using *mantel* function with 999 permutations using environmental distances extracted from *bioenv* results (vegan package, Oksanen et al., 2020).

Results

Environmental conditions

Subsurface streambed temperatures in both runs and the upper riffle of the HG reach were typically between 16 and 18 °C, with some patches of cooler water (14 – 16 °C; Fig. 2a). The lower HG riffle was cooler with temperatures largely between 14 – 16 °C, with small areas as low as 12 °C). The upper run in the MG reach had uniform subsurface streambed temperature of 14 – 16 °C, whereas the two riffles (10 to 18 °C) and more downstream run (12 – 16 °C) had more spatially variable subsurface streambed temperatures (Fig. 2b). The LG reach had the warmest subsurface temperatures that were typically greater than 16 °C (Fig. 2c).

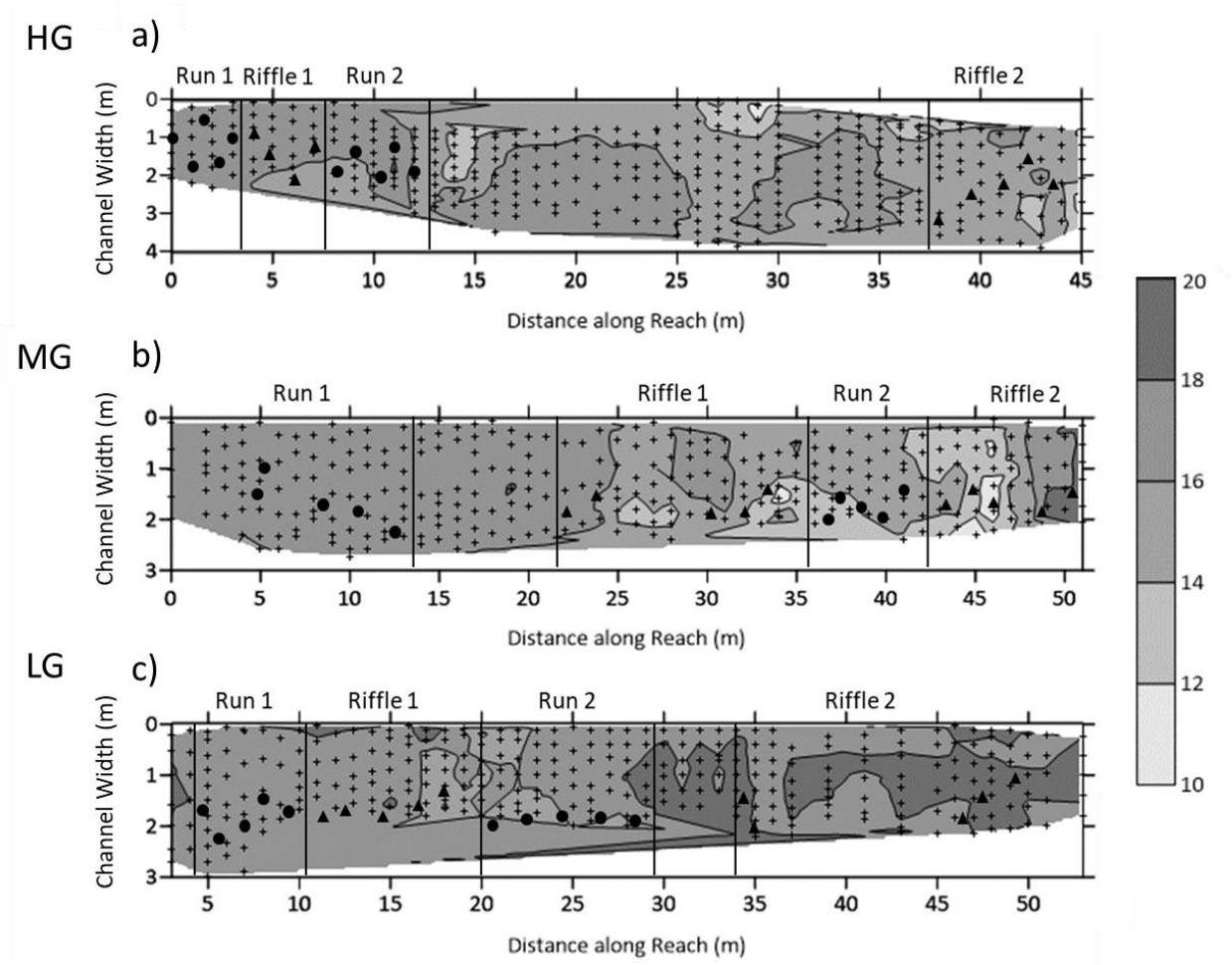

Fig. 2 Subsurface (10 cm) streambed temperatures (°C) for three reaches in Kintore Creek, Ontario, Canada receiving high (HG, a), moderate (MG, b), and low (LG, c) inputs of groundwater. The temperature surface was generated by kriging interpolation. Cross symbols identify temperature measurement locations. Black circles show tile placement in runs, black triangles show tile placement in riffles.

The temperature gradient (stream surface water temperature – subsurface streambed temperature) in the HG reach increased from the top to bottom of the reach (Fig. 3a). The upper run temperature gradients were between 1 and 3 °C, the upper riffle and lower run ranged from 1 to 7 °C, whereas the lower riffle was typically between 5 and 9 °C. The temperature gradient of the upper run in the MG reach was consistently between -1 and 1 °C (Fig. 3b). In contrast, the lower run and both riffles were patchier, exhibiting areas of lower (1 – 3 °C) and higher (5 – 7 °C) temperature gradients. Throughout the LG reach, the temperature gradients were typically

between 1 and 3 °C, with small patches of larger temperature gradients (3 – 5 °C) in the upper riffle and lower run (Fig. 3a).

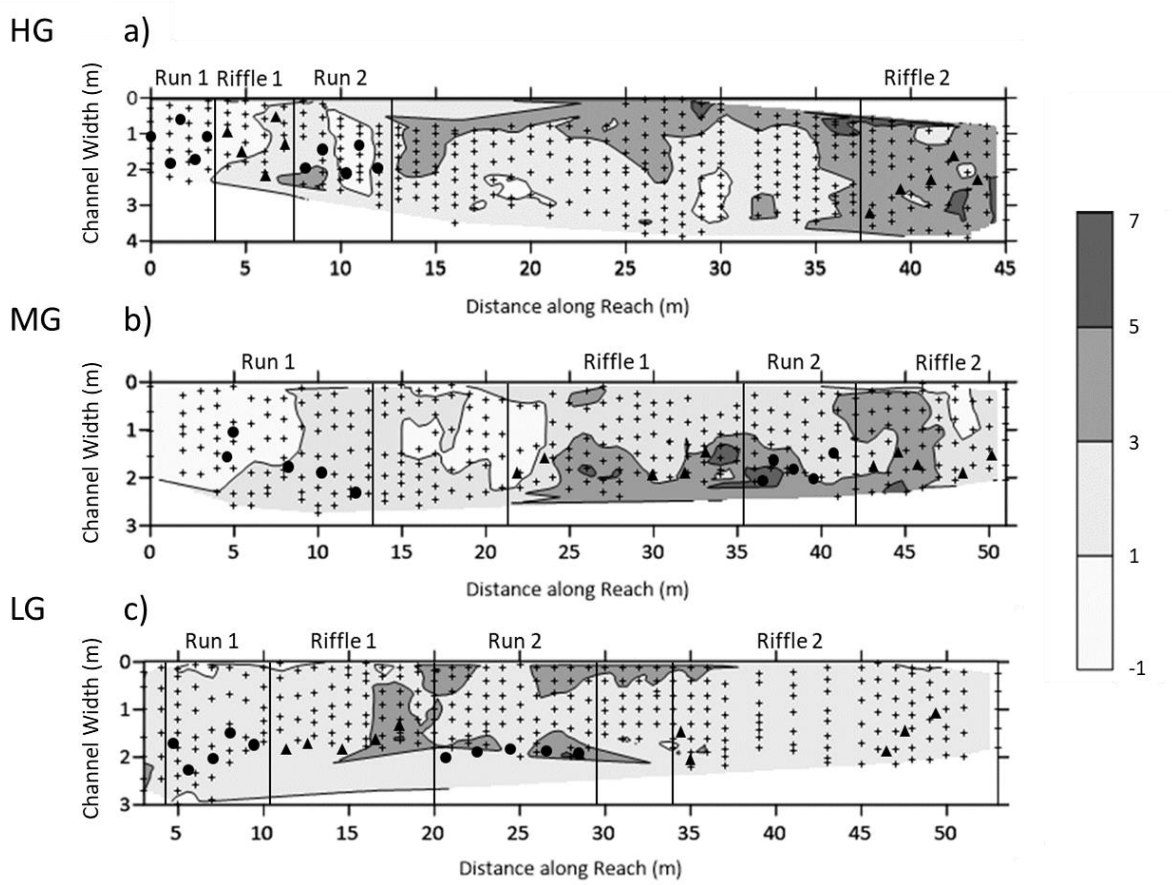

Fig. 3 Temperature gradient between surface water and subsurface streambed temperature (°C) (i.e., stream surface water temperature - subsurface streambed temperature) for three reaches in Kintore Creek, Ontario, Canada receiving high (HG, a), moderate (MG, b), and low (LG, c) inputs of groundwater. The temperature surface was generated by kriging interpolation. Cross symbols identify temperature measurement locations. Black circles show tile placement in runs, black triangles show tile placement in riffles.

Across all riffle habitats, stream velocity in runs (0.120 ± 0.059 m/s) was about 60% of that of riffles (0.217 ± 0.096 m/s) (Fig. 4a). MG had the fastest mean stream velocity in riffles and slowest in runs. Runs (15.8 ± 5.6 cm) were typically deeper than riffles (11.4 ± 2.5 cm) across all reaches (Fig. 4b), with LG having the smallest depths for both habitats and the smallest difference between runs and riffles (~3 cm on average).

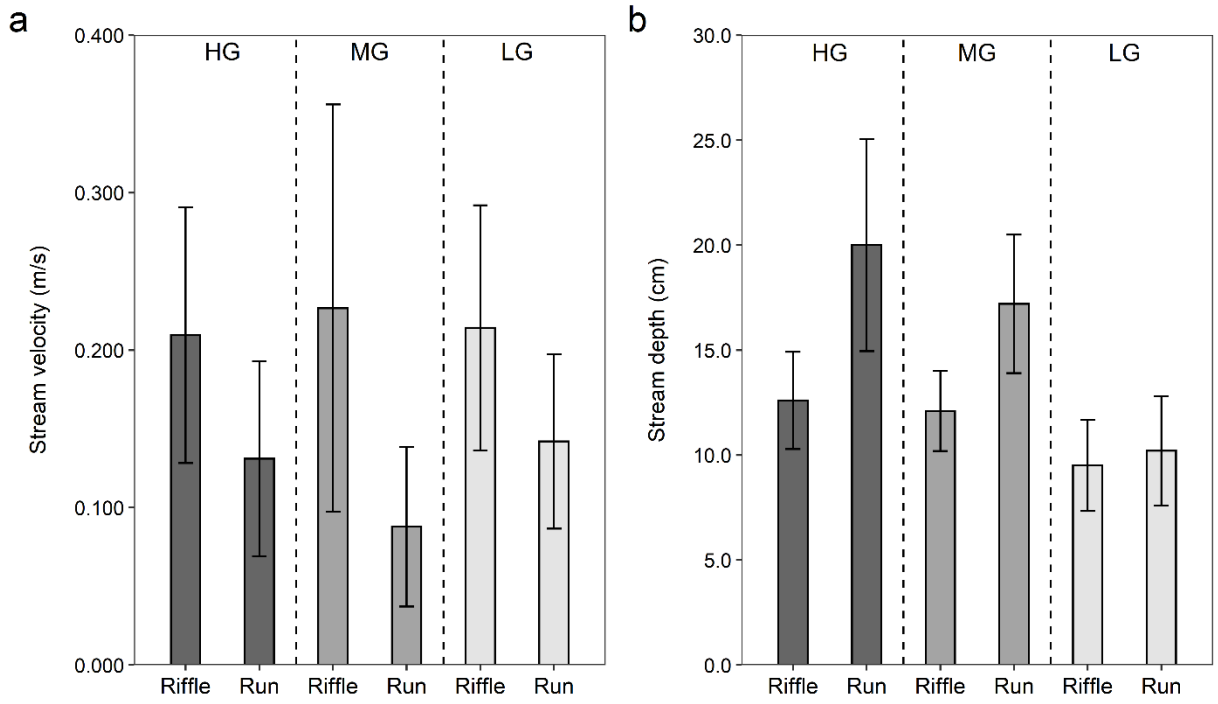

Fig. 4 Bar plots (mean ± one standard deviation) of (a) stream velocity (m/s) and (b) stream depth (cm) for riffle (n = 10) and run (n = 10) habitats in three sampled stream reaches (high groundwater reach [HG], moderate groundwater reach [MG], and low groundwater reach [LG]) in Kintore Creek, Ontario.

Across all reaches and habitats, mean daily surface water temperature ranges and mean daily surface water temperatures were within approximately 2.5 °C and 2 °C, respectively (Fig. 5). The greatest mean daily temperature range for both habitats was observed in HG (Fig. 5a). Mean daily temperature was the lowest in HG for both habitats (Fig. 5b).

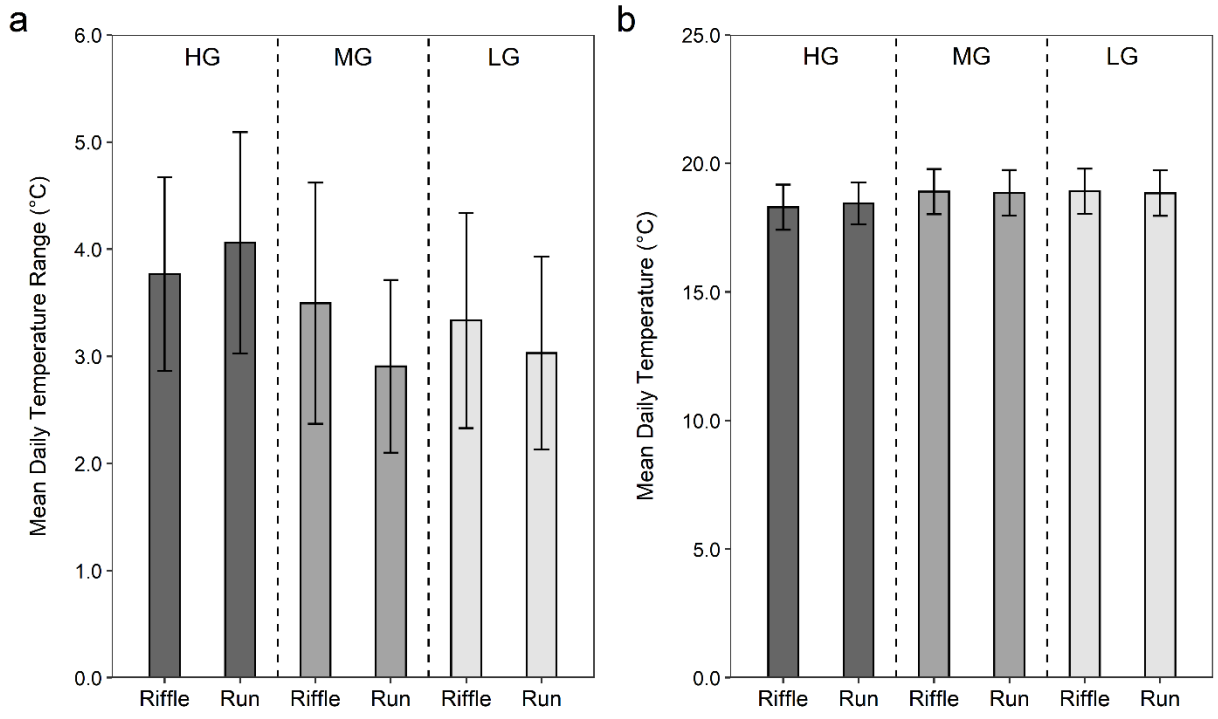

Fig. 5 Bar plots (mean ± one standard deviation) of (a) mean daily temperature range (°C) and (b) mean daily temperature (°C) of stream water temperature for riffle (n = 10) and run (n = 10) habitats in each study reach (high groundwater reach [HG], moderate groundwater reach [MG], and low groundwater reach [LG]) in Kintore Creek, Ontario.

Reach and habitat effects on biofilms and cellulose decomposition

The GLM assessing spatial patterns in chl-*a* found the interaction of reach and habitat was significant ($F_{2,54}$ = 2.66, p = 0.08) (Fig. 6a). Tukey's post-hoc tests showed three-times greater accumulation in runs than riffles in HG (p = 0.07). Similarly, chl-*a* accumulation in runs at MG was approximately five-times greater than in riffles (p = 0.01). However, no differences were found between chl-*a* accumulation in riffles and runs at LG (p = 0.99).

The GLM on biofilm growth rate identified a significant interaction of groundwater input and habitat ($F_{2,54}$ = 2.64, p = 0.08) (Fig. 6b). Runs in HG had biofilm growth rates more than double that of riffles (p = 0.04). Similarly, runs in MG had biofilm growth rates more than three-

times greater than riffles (p = 0.02). In contrast, runs in LG had biofilm growth rates that were not different than those in riffles (p = 0.99).

The PLS regressions for biomass metrics (chl-*a* accumulation and biofilm growth rate) resulted in an interpretable model (Q^2 = 0.277) with one component. The component explained 45 % of the variance of the environmental variables and 34 % of the variance in biological variables. The component organized sites based on variation in stream velocity (VIP = 1.12) and depth (VIP = 1.38). Depth was positively associated with chl-*a* accumulation and biofilm growth rate. Conversely, stream velocity was negatively associated with chl-*a* accumulation and biofilm growth rate. Run samples from HG were located towards the positive end of the axis. All other samples were clustered in the center-left of the axis.

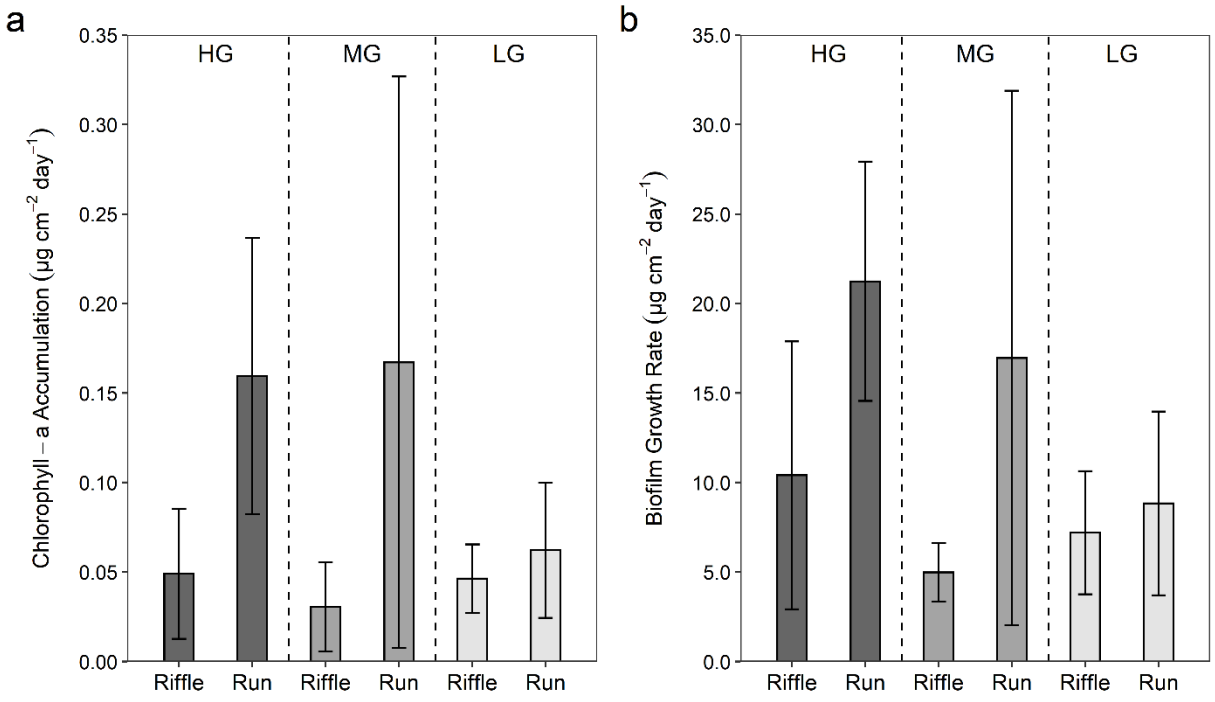

Fig. 6 Bar plots (mean ± one standard deviation) of (a) chl-*a* accumulation (µg cm^{-2} day^{-1}) and (b) biofilm growth rate (µg cm^{-2} day^{-1}) for riffle (n = 10) and run (n = 10) habitat units in each study reach (high groundwater reach [HG], moderate groundwater reach [MG], and low groundwater reach [LG]) in Kintore Creek, Ontario.

Diatom Assemblages

Fifty-four diatom species were observed across all reaches and habitat units. The three most abundant taxa *Achnanthidium eutrophilum* (Lange-Bertalot 1999) Lange-Bertalot (20 %),

Amphora pediculus (Kützing) Grunow (14 %), and *Cocconeis placentula* (Ehrenberg) (52 %) accounted for 86 % of total abundance across all reaches. Total taxa richness in HG was 33 in runs and 29 in riffles. At MG, richness was 22 in runs and 22 in riffles. From riffles to runs, *C. placentula* abundance decreased by two-thirds and *A. eutrophilum* abundance increased by about a third. In LG, total taxa richness was 25 in runs and 25 in riffles. Both riffles and runs in LG were dominated by *C. placentula*.

GLM analyses of taxa richness, % dominant, taxa evenness, and density of diatoms showed differing responses to the effects of groundwater input and habitat (Fig. 7). For taxa richness, there was a significant interaction of groundwater input and habitat ($F_{1,24} = 5.98$, $p = 0.005$) (Fig. 7a). However, there were no differences between habitats in HG ($p = 0.29$), MG ($p = 0.13$), or LG ($p = 0.87$). For % dominant, there was also a significant interaction of groundwater input and habitat ($F_{1,24} = 3.81$, $p = 0.03$) (Fig. 7b). There were more % dominant taxa in runs compared to riffles in MG ($p = 0.04$), but no difference in HG ($p = 0.99$) or LG ($p = 0.99$). Analysis of taxa evenness showed a non-significant interaction term ($p = 0.68$), and no effect of habitat ($p = 0.35$), but there was a difference among groundwater input levels ($F_{2,24} = 4.45$, $p = 0.02$) (Fig. 7c). Taxa evenness was greater in HG compared to MG ($p = 0.014$), but there were no differences between HG and LG ($p = 0.63$) nor MG and LG ($p = 0.12$). Diatom slide density had a significant interaction of groundwater input and habitat ($F_{1,24} = 4.07$, $p = 0.02$) (Fig. 7d). Diatom density was greater in run than in riffle habitats in HG ($p = 0.006$) and MG ($p = 0.06$), but there was no difference between habitats in LG ($p = 0.99$).

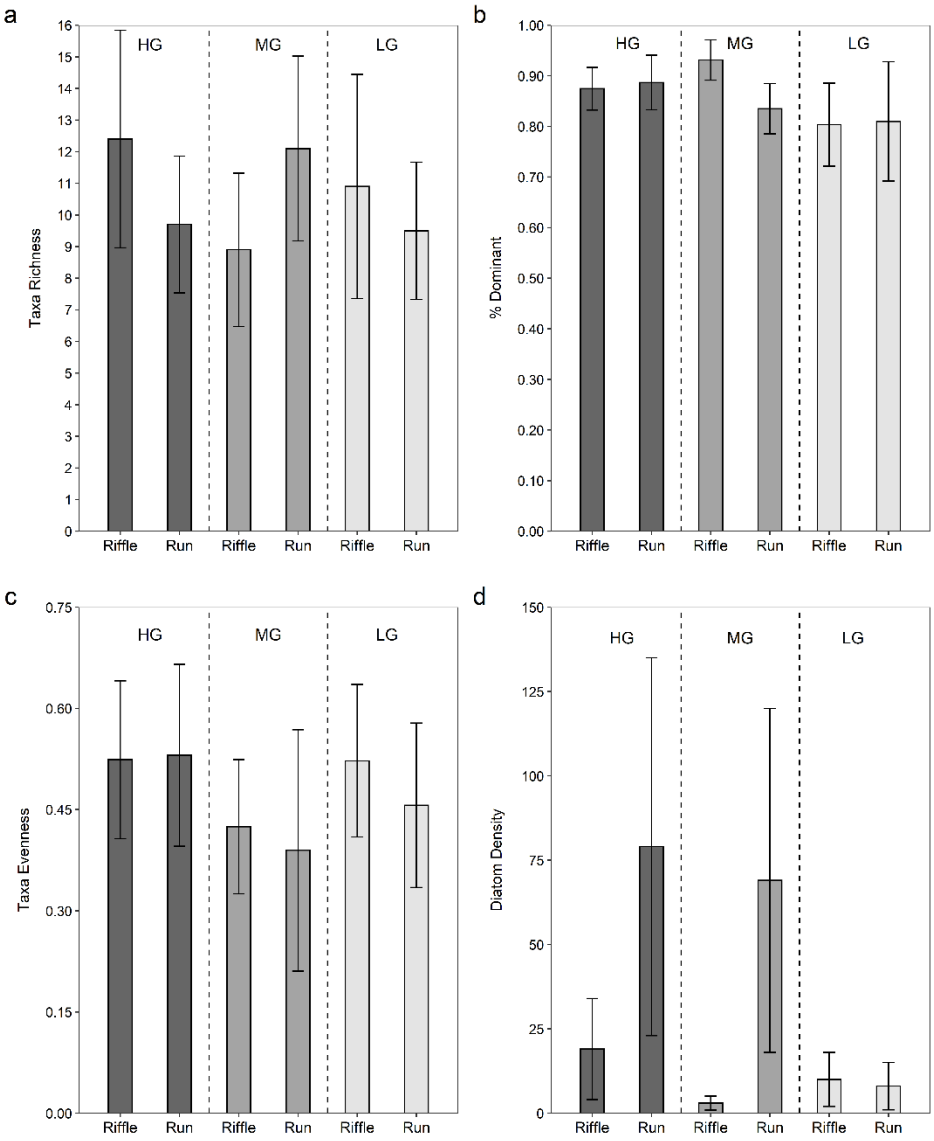

Fig. 7 Barplots (mean ± one standard deviation) for (a) taxa richness (b) % dominant (c) evenness and (d) density of diatom for riffle (n = 10) and run (n = 10) habitat units in three study (high groundwater reach [HG], moderate groundwater reach [MG], and low groundwater reach [LG]) in Kintore Creek, Ontario.

Ordination of relative abundance of diatom assemblages showed that diatom communities in riffles and runs in HG clustered separately from those in MG and LG (Fig. 8). A two factor PERMANOVA showed a significant interaction between reaches of varying groundwater input and habitat (pseudo-$F_{(2,54)}$ = 2.10, p = 0.03). A post-hoc pairwise comparison of habitats with

groundwater input showed that diatom assemblages in riffles and runs differed significantly in HG ($p = 0.005$) and MG ($p = 0.006$), but not in LG ($p = 0.28$). *C. placentula* abundance decreased by a third from riffles to runs, whereas *A. eutrophilum* abundance increased from negligible (< 2 %) in riffles to a quarter of total abundance in runs.

SIMPER analysis indicated that nearly three-quarters of total average dissimilarity (32.3 %) between runs and riffles in HG were attributed to six taxa: *C. placentula* (22.3 %), *A. eutrophilum* (14.4 %), *A. pediculus* (14.2 %), *Reimeria sinuata* (W. Gregory) Kociolek & Stoermer (6.0 %), and *Planothidium frequentissimum* (Lange-Bertalot) Lange-Bertalot (5.6 %). In MG, total average dissimilarity between runs and riffles was 36.0 %, with five taxa: *A. eutrophilum* (20.2 %), *C. placentula* (19.0 %), *A. pediculus* (12.5 %), *P. frequentissimum* (9.9 %), and *Cocconeis pediculus* (Ehrenberg 1838) (5.7 %) contributing two-thirds of total average dissimilarity. BIOENV analysis showed that depth and pH were positively correlated ($r = 0.504$, $p = 0.001$) with dissimilarity among diatom assemblages (Fig. 8).

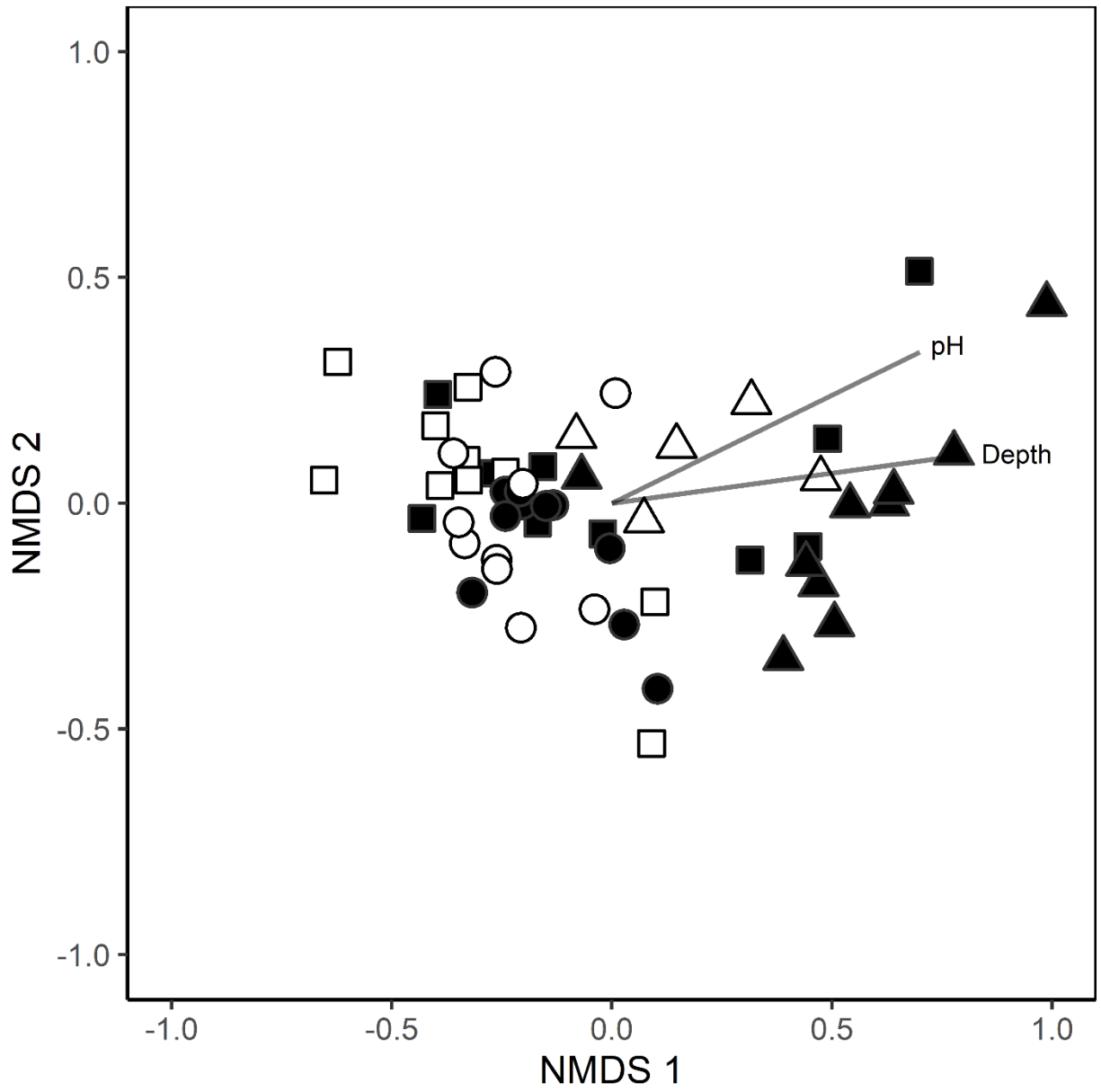

Fig. 8 nMDS ordination plot using Bray-Curtis dissimilarity index showing separation of diatom assemblage relative abundance based on reach and habitat (stress = 0.12) with significant (r = 0.504, p = 0.001) environmental variables vectors overlaid. Reaches are represented by shape where triangles are high groundwater reach (HG), squares are moderate groundwater reach (MG), and circles are low groundwater reach (LG). Habitats are represented by open shapes for riffles and closed shapes for runs.

Cellulose Decomposition

Across all reaches and habitats, mean % tensile loss per day (% tensile loss day^{-1}) at the streambed surface was 1 to 2 % per day faster than in the subsurface (Fig. 9). The LMEM assessing differences in % tensile loss day^{-1} at the streambed surface showed a significant interaction between groundwater input and habitat ($F_{1,24} = 12.59$, $p < 0.001$). Subsequent GLMs showed that rates of % tensile loss day^{-1} in riffles were 1.15-times faster than runs ($p < 0.001$). Rates of % tensile loss day^{-1} in riffles in HG were 10% faster than runs in HG ($p = 0.002$). Similarly, in MG rates of % tensile loss day^{-1} in riffles a third faster than runs ($p = 0.006$). However, % tensile loss day^{-1} did not differ between riffles and runs in LG ($p = 0.50$).

The PLS analysis for streambed surface % tensile loss produced an interpretable model ($Q^2 = 0.272$) comprised of one component. The component accounted for 44 % of the variance in environmental variables with stream velocity (VIP = 1.01), mean daily temperature range (VIP = 1.22), and mean daily temperature (VIP = 1.18) retained. The component also explained 34 % of the variance in streambed surface % tensile loss day^{-1}. Stream velocity, mean daily temperature range, and mean daily temperature were positively associated with surface % tensile loss day^{-1}. In HG and MG, riffle samples were typically clustered on the positive end of the axis. Runs from all reaches and riffles from LG tended to cluster in the center and center-left of the axis.

The LMEM on subsurface tensile loss showed no interaction between groundwater input and habitat ($F_{2,24} = 0.18$, $p = 0.84$), as well as no effect of habitat ($F_{1,24} = 0.69$, $p = 0.42$) (Fig. 9a). There was an effect of groundwater input ($F_{2,24} = 3.74$, $p = 0.04$), such that subsurface tensile loss was faster at HG than at either MG ($p = 0.02$) and LG ($p = 0.002$) (Fig. 9b). There was no difference in subsurface tensile loss between MG and LG ($p = 0.70$).

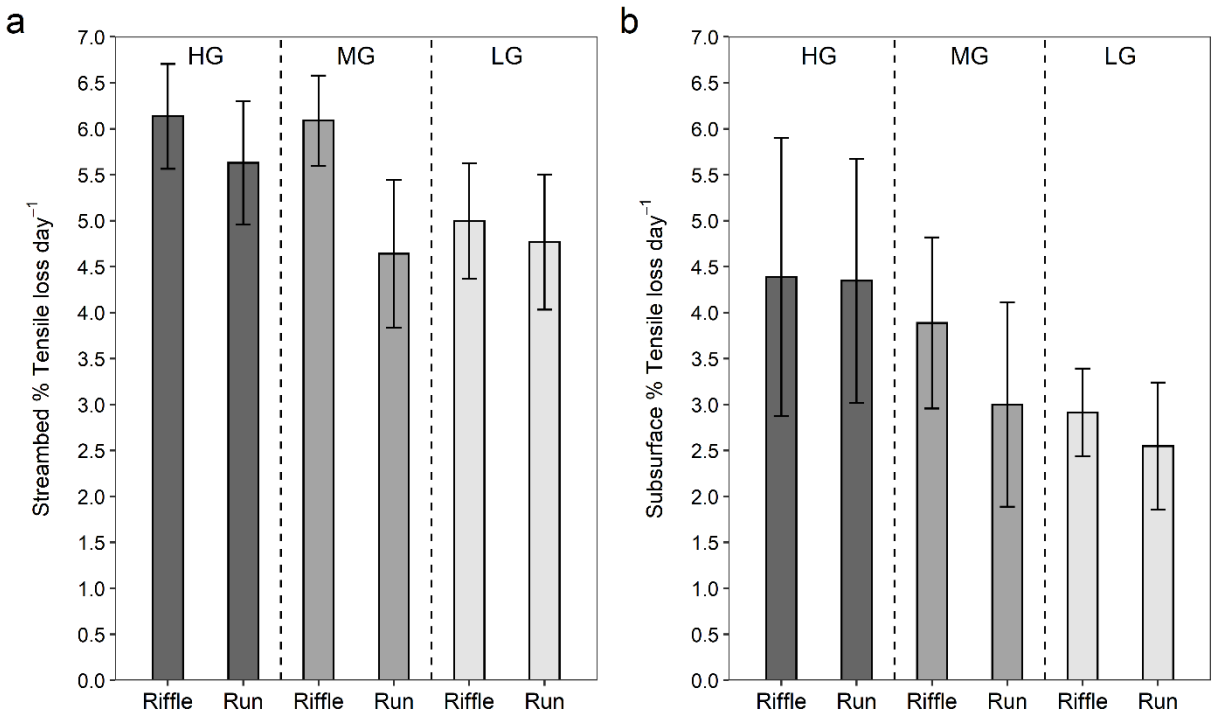

Fig. 9 Bar plots (mean ± one standard deviation) for (a) surface cellulose decomposition (% tensile loss day^{-1}) for riffle (n = 50) and run (n = 50) habitats, and (b) subsurface cellulose decomposition (% tensile loss day^{-1}) for riffle (n = 30) and run (n = 30) habitat units in three study reaches (high groundwater reach [HG], moderate groundwater reach [MG], and low groundwater reach [LG]) in Kintore Creek, Ontario.

Discussion

Habitat specificity of groundwater effects on stream biofilms

Biofilm biomass, diatom assemblage composition, and cellulose decomposition differed among reaches in Kintore Creek with greater chl-*a* accumulation and biofilm growth in reaches receiving moderate and high groundwater inputs. Greater biomass in groundwater receiving reaches is consistent with past findings from a range of stream ecosystem types. For example, in an alluvial river in northwestern Montana groundwater input was typically associated with increased chl-*a* and biomass (Stanford et al., 1994; Wyatt et al., 2008). Similarly, algal biomass in an alpine stream was greater downstream of a groundwater spring (Roy et al., 2011). Likewise, groundwater inputs promoted algal production in the Fitzroy River, Australia (Burrows et al., 2020). Past work has also found evidence that groundwater inputs influence

diatom assemblage composition. Indeed, Roy et al. (2011) and Stevenson et al. (2009) both observed stream reaches with significant groundwater inputs to exhibit compositionally distinct diatom assemblage composition compared to stream reaches not receiving groundwater. Additionally, past work has shown that groundwater inputs are associated with slower cellulose decomposition rates in warmer seasons (Griffiths & Tiegs, 2016; Poisson & Yates, 2022). However, unlike many past studies, our study found that effects of groundwater were habitat specific.

Many of the ecological endpoints assessed in our study were indicative of an interactive effect of groundwater input and habitat. Indeed, we found that runs in reaches with moderate to high groundwater input had 2-3 times greater chl-*a* accumulation and biofilm growth rates, as well as greater diatom density than associated riffles. Likewise, diatom composition shifted in dominant taxa from *C. placentula* in riffles to *A. eutrophilum* in runs. Finally, we found that rates of tensile loss at the streambed surface (but not buried) were greater in the reach with high groundwater inputs. Thus, it appears that stream biofilm communities at the streambed experience effects of groundwater inputs differently based on habitat type.

Habitat specific manifestation of groundwater effects is consistent with known groundwater – surface water exchange patterns (i.e., upwelling and downwelling) in riffles and runs. At the beginning of riffles, downward pressure has been shown to result in surface water downwelling, followed by groundwater upwelling at the end of the riffle or start of the subsequent run (Thibodeaux & Boyle, 1987; Harvey & Bencala, 1993). Thus, groundwater inputs may have been suppressed in riffles but expressed in runs, leading to the habitat specific outcomes we observed. However, as suppression of groundwater inputs to riffles is not fully supported by the subsurface temperature measures, other microscale factors (e.g., chemical constituents, redox) may also be important in determining the observed ecological patterns that manifested at the habitat scale. Future work that directly captures the amount and characteristics (e.g., nutrient concentrations) of upwelling groundwater are thus needed to validate the role of habitat type as a modifier of groundwater – surface water exchange patterns and provide a mechanistic link between groundwater input and stream biofilm communities.

Although biological patterns matched expected associations between habitat type and effects of groundwater inputs, these differences also corresponded to patterns of stream velocity

in the groundwater receiving reaches. As stream velocity has been well-demonstrated to influence algal biomass, diatom assemblage composition, and cellulose decomposition (Horner et al., 1990; Biggs & Gerbeaux, 1993; Biggs & Hickey, 1994; Biggs et al., 1998; Tiegs et al., 2009; Webb et al., 2019), it is possible that velocity may have partially accounted for the patterns we observed. Indeed, a modifying role of stream velocity on groundwater inputs was reported by Burrows et al. (2020) who suggested that greater environmental stability in areas of slower velocity coupled with enhanced delivery of resources (e.g., chemical constituents, nutrients, and thermal effects) via groundwater input cumulatively acted to enhance algal biomass accumulation. Differences in stream velocity may have also impacted diatom community composition, as diatoms have shown varying preferences to velocity (Van Dam et al., 1994; Passy, 2007). Conversely, faster velocities and greater sheer stress in riffles compared to runs may more rapidly dissipate the effects of groundwater inputs close to the streambed surface (Storey et al., 2003). Cumulative effects of stream velocity and moderate to high groundwater input are also consistent with the patterns of cellulose decomposition we observed as the increased velocity and associated enhancement of physical breakdown may have further accelerated decomposition in riffles (Tiegs et al., 2009; Webb et al., 2019). However, it is unlikely that the observed biological patterns were solely because of velocity. We base this conclusion on our finding no biological differences between habitat types in the low groundwater reach, despite this reach exhibiting similar velocity patterns to the moderate and high groundwater reaches. Our results suggest that the role of stream velocity is, at most, subsidiary to that of groundwater, and therefore additional studies are needed to test hypotheses regarding the apparent cumulative effects of groundwater input and stream velocity.

Groundwater modified environmental drivers of stream biofilms

Although we detected a relationship between stream biofilm metrics and groundwater input, we did not observe associations between measured stream environmental parameters that can be modified by groundwater and the observed ecological heterogeneity. The lack of association between ecological endpoints and measured environmental parameters in reaches of Kintore Creek is in contrast with past studies in low nutrient streams (i.e., < 5 μg P L^{-1} SRP, < 0.50 mg N L^{-1} NO_3-N) that have suggested that groundwater inputs were associated with greater benthic algal biomass and heterotrophic microbial activity (Wyatt et al., 2008; Roy et al., 2011;

Fellman et al., 2014; Griffiths & Tiegs, 2016; Mejia et al., 2016; Burrows et al., 2020). The difference in our results compared to past studies may be due to reaches in our study having more or similar amounts of nutrients in the surface water compared to groundwater inputs (C. Robinson, unpublished data). Likewise, we found that mean daily temperature of stream water at the bed was 18 °C and varied by approximately 2 °C across all reaches and habitats, despite indications from temperature mapping of significant groundwater flux in the high and moderate groundwater reaches. As previous work has suggested that differences in temperature need to be at least 3 °C and 4 – 5 °C, to impact chl-*a* and cellulose decomposition, respectively (Godwin & Carrick, 2008; Griffiths & Tiegs, 2016; Delgado et al., 2017; Follstad Shah et al., 2017), it appears groundwater inputs were insufficient to affect stream biota through control of stream temperatures. Indeed, the lack of among reach variation in nutrients and temperature suggests that impacts of groundwater inputs may have been masked by prevailing surface water conditions.

Streambed temperature mapping of the three reaches of Kintore Creek indicated patchiness in groundwater input within the high and moderate groundwater reaches. However, the observed spatial patterns of groundwater inputs were not detectable at the reach or habitat unit scales with the approaches we used to measure to environmental conditions where biofilms were sampled. Thus, it appears that in Kintore Creek, effects of groundwater inputs may have been rapidly dissipated at the streambed – surface water interface. Alternatively, the ecological response observed in groundwater receiving reaches may have been due to unaccounted environmental differences among reaches rather than groundwater inputs. However, this second explanation is unlikely as we found that reaches with high and moderate groundwater input showed similar ecological patterns. Rather, our findings of biological variation among reaches, without associations to reach scale environmental conditions, suggest that stream biofilm communities and cellulose breakdown may have been more strongly linked to microscale environmental conditions at the stream water – biofilm interface. However, measuring environmental conditions at such microscales is a methodologically challenging endeavour and was beyond the scope of this study. Future studies using novel methods to capture environmental conditions at the stream water – biofilm interface are thus needed to further our understanding of the role of groundwater inputs in structuring stream communities and processes.

Effect of burial on cellulose decomposition

We observed strips on the streambed surface generally had faster breakdown rates than strips buried in the substrate; a finding consistent with past studies (Boulton & Quinn, 2000; Claret et al., 2001; Cornut et al., 2010). Slower subsurface cellulose breakdown in the streambed has been attributed to reduced physical abrasion, as well as lower temperature and dissolved oxygen limiting heterotrophic activity in the hyporheic zone (Strommer & Smock, 1989; Malard & Hervant, 1999; Crenshaw et al., 2002; Cornut et al., 2010). The differences in decomposition between the streambed surface and subsurface highlight the need for measurement of both surface and subsurface decomposition to fully describe rates of organic matter processing in streams.

For subsurface cellulose breakdown, we found that the reach with high groundwater input was associated with faster subsurface cellulose breakdown compared to the moderate and low groundwater reaches. Our results are in contrast to past work that suggest that higher groundwater inputs would slow subsurface decomposition due to cooler water temperatures and lower dissolved oxygen (Štěrba et al., 1992; Boulton & Foster, 1998; Franken et al., 2001). A potential explanation is that greater groundwater – surface water exchange in the high groundwater reach may have stimulated heterotrophic decomposers in the streambed through greater access to key biogeochemical resources (e.g., DOC, nutrients). However, because we did not sample subsurface conditions (e.g., dissolved oxygen) aside from temperature, our study is limited in explaining the observed patterns. Thus, future studies should focus on investigating the controls of organic matter breakdown in the subsurface when varying amount of groundwater is present.

Summary

We found that the ecological response to groundwater input manifested in specific habitat types and varied depending on the biological measure. In reaches receiving moderate to high groundwater inputs, biofilm biomass was greater in runs, and streambed cellulose breakdown was faster in riffles. However, ecological patterns were not associated with our measurements of surface water temperature or nutrient availability, suggesting that some controlling factors were not measured (e.g., chemical characteristics of upwelling groundwater), or that impacts of groundwater inputs may have dissipated rapidly at the streambed interface, and thus were not

captured by our environmental measurements. Indeed, we suspect that the effect of groundwater inputs may be limited to streambed surface interface, where biofilms experience and interact with the stream environment. Future work on the effect of groundwater inputs on stream biofilm communities and cellulose decomposition in enriched streams should focus on assessments in multiple habitat types and environmental measurements at the stream water – biofilm interface.

References

Agricutlure and Agri-Food Canada, 2020. AAFC annual crop inventory 2019.

Atkinson, A. P., I. Cartwright, B. S. Gilfedder, H. Hofmann, N. P. Unland, D. I. Cendón, & R. Chisari, 2015. A multi-tracer approach to quantifying groundwater inflows to an upland river; assessing the influence of variable groundwater chemistry. Hydrological Processes 29: 1–12, https://doi.org/10.1002/hyp.10122.

Bates, D., M. Mächler, B. M. Bolker, & S. C. Walker, 2015. Fitting linear mixed-effects models using lme4. Journal of Statistical Software. https://doi.org/10.18637/jss.v067.i01.

Battin, T. J., K. Besemer, M. M. Bengtsson, A. M. Romani, & A. I. Packmann, 2016. The ecology and biogeochemistry of stream biofilms. Nature Reviews Microbiology 14: 251–263, https://doi.org/10.1038/nrmicro.2016.15.

Battin, T. J., L. A. Kaplan, J. D. Newbold, & C. M. E. Hansen, 2003. Contributions of microbial biofilms to ecosystem processes in stream mesocosms. Nature 426: 439–442, https://doi.org/10.1038/nature02152.

Benfield, E. F., K. M. Fritz, & S. D. Tiegs, 2017. Leaf-Litter Breakdown In Lamberti, G. A., & F. R. Hauer (eds), Methods in Stream Ecology, Volume 2: Ecosystem Function. Elsevier, Academic Press: 71–82, https://doi.org/10.1016/B978-0-12-813047-6.00005-X.

Besemer, K., 2015. Biodiversity, community structure and function of biofilms in stream ecosystems. Research in Microbiology 166: 774–781, https://doi.org/10.1016/j.resmic.2015.05.006.

Bey, M., & L. Ector, 2013. Atlas des diatomées des cours d'eau de la région Rhône-Alpes − Tomes 1 à 6. DREAL, Rhône-Alpes.

Biggs, B. J. F., 1995. The contribution of flood disturbance, catchment geology and land use to the habitat template of periphyton in stream ecosystems. Freshwater Biology 33: 419–438, https://doi.org/10.1111/j.1365-2427.1995.tb00404.x.

Biggs, B. J. F., & P. Gerbeaux, 1993. Periphyton development in relation to macro-scale (geology) and micro-scale (velocity) limiters in two gravel-bed rivers , New Zealand. New

Zealand Journal of Marine and Freshwater Research 27: 39–53, https://doi.org/10.1080/00288330.1993.9516544.

Biggs, B. J. F., D. G. Goring, & V. I. Nikora, 1998. Subsidy and stress responses of stream periphyton to gradients in water velocity as a function of community growth form. Journal of Phycology 34: 598–607, https://doi.org/10.1046/j.1529-8817.1998.340598.x.

Biggs, B. J. F., & C. W. Hickey, 1994. Periphyton responses to a hydraulic gradient in a regulated river in New Zealand. Freshwater Biology John Wiley & Sons, Ltd 32: 49–59, https://doi.org/https://doi.org/10.1111/j.1365-2427.1994.tb00865.x.

Biggs, B. J. F., V. I. Nikora, & T. H. Snelder, 2005. Linking scales of flow variability to lotic ecosystem structure and function. River Research and Applications 21: 283–298, https://doi.org/10.1002/rra.847.

Boano, F., J. W. Harvey, A. Marion, A. I. Packman, R. Revelli, L. Ridolfi, & A. Wörman, 2014. Hyophreic flow and transport processes. Reviews of Geophysics 52: 603–679, https://doi.org/10.1002/2012RG000417.

Borchardt, M., 1996. Nutrients In Stevenson, R. J., M. Bothwell, & R. Low (eds), Algal ecology: freshwater benthic ecosystems. Academic Press, San Diego, CA, USA: 183–227.

Boulton, A. J., & J. G. Foster, 1998. Effects of buried leaf litter and vertical hydrologic exchange on hyporheic water chemistry and fauna in a gravel-bed river in northern New South Wales, Australia. Freshwater Biology 40: 229–243, https://doi.org/10.1046/j.1365-2427.1998.00345.x.

Boulton, A. J., & P. J. Hancock, 2006. Rivers as groundwater-dependent ecosystems: A review of degrees of dependency, riverine processes and management implications. Australian Journal of Botany 54: 133–144, https://doi.org/10.1071/BT05074.

Boulton, A. J., & J. M. Quinn, 2000. A simple and versatile technique for assessing cellulose decomposition potential in floodplain and riverine sediments. Archiv für Hydrobiologie 150: 133–151, https://doi.org/10.1127/archiv-hydrobiol/150/2000/133.

Brunke, M., & T. Gonser, 1997. The ecological significance of exchange processes between rivers and groundwater. Freshwater Biology 37: 1–33, https://doi.org/10.1046/j.1365-2427.1997.00143.x.

Burrows, R. M., L. Beesley, M. M. Douglas, B. J. Pusey, & M. J. Kennard, 2020. Water velocity and groundwater upwelling influence benthic algal biomass in a sandy tropical river: implications for water-resource development. Hydrobiologia 847: 1207–1219, https://doi.org/10.1007/s10750-020-04176-3.

Carrascal, L. M., I. Galván, & O. Gordo, 2009. Partial least squares regression as an alternative to current regression methods used in ecology. Oikos 118: 681–690, https://doi.org/10.1111/j.1600-0706.2008.16881.x.

Clapcott, J. E., & L. A. Barmuta, 2010. Metabolic patch dynamics in small headwater streams: Exploring spatial and temporal variability in benthic processes. Freshwater Biology 55: 806–824, https://doi.org/10.1111/j.1365-2427.2009.02324.x.

Claret, C., A. J. Boulton, M.-J. Dole-Olivier, & P. Marmonier, 2001. Functional processes versus state variables: interstitial organic matter pathways in floodplain habitats. Canadian Journal of Fisheries and Aquatic Sciences 58: 1594–1602, https://doi.org/10.1139/cjfas-58-8-1594.

Clarke, K. R., & R. N. Gorley, 2015. Primer v7: User manual/tutorial. Primer-E. Plymouth, UK, 93.

Clarke, K. R., & R. M. Warwick, 1994. Similarity-based testing for community pattern: the two-way layout with no replication. Marine Biology 118: 167–176, https://doi.org/10.1007/BF00699231.

Coleman, R. L., & C. N. Dahm, 1990. Stream geomorphology: effects on periphyton standing crop and primary p roduction. Journal of the North American Benthological Society 9: 293–302, https://doi.org/10.2307/1467897.

Conant, B., C. E. Robinson, M. J. Hinton, & H. A. J. Russell, 2019. A framework for conceptualizing groundwater-surface water interactions and identifying potential impacts on water quality, water quantity, and ecosystems. Journal of Hydrology 574: 609–627, https://doi.org/10.1016/j.jhydrol.2019.04.050.

Cook, P. G., 2013. Estimating groundwater discharge to rivers from river chemistry surveys. Hydrological Processes 27: 3694–3707, https://doi.org/10.1002/hyp.9493.

Cornut, J., A. Elger, D. Lambrigot, P. Marmonier, & E. Chauvet, 2010. Early stages of leaf

decomposition are mediated by aquatic fungi in the hyporheic zone of woodland streams. Freshwater Biology 55: 2541–2556, https://doi.org/10.1111/j.1365-2427.2010.02483.x.

Crenshaw, C. L., H. M. Valett, & J. L. Tank, 2002. Effects of coarse particulate on fungal biomass and organic matter in invertebrate the of subsurface a headwater stream density. Journal of the North American Benthological Society 21: 28–42, https://doi.org/https://doi.org/10.2307/1468297.

Cummins, K. W., 1974. Structure and Function of Stream Ecosystems. BioScience 24: 631–641, https://doi.org/https://doi.org/10.2307/1296676.

Delgado, C., S. F. P. Almeida, C. L. Elias, V. Ferreira, & C. Canhoto, 2017. Response of biofilm growth to experimental warming in a temperate stream. Ecohydrology 10: 1–9, https://doi.org/10.1002/eco.1868.

Dent, C. L., N. B. Grimm, & S. G. Fisher, 2001. Multiscale effects of surface-subsurface exchange on stream water nutrient concentrations. Journal of the North American Benthological Society 20: 162–181, https://doi.org/10.2307/1468313.

Environment and Climate Change Canada, 2010. Canadian Climate Normals. .

Eriksson, L., T. Bryne, E. Johansson, J. Trygg, & C. Wiksröm, 2013. Multi-and megavariate data analysis: part I: basic principles and applications. Umetrics AB, Umeå.

Fellman, J. B., R. G. M. Spencer, P. A. Raymond, N. E. Pettit, G. Skrzypek, P. J. Hernes, & P. F. Grierson, 2014. Dissolved organic carbon biolability decreases along with its modernization in fluvial networks in an ancient landscape. Ecology 95: 2622–2632, https://doi.org/10.1890/13-1360.1.

Follstad Shah, J. J., J. S. Kominoski, M. Ardón, W. K. Dodds, M. O. Gessner, N. A. Griffiths, C. P. Hawkins, S. L. Johnson, A. Lecerf, C. J. LeRoy, D. W. P. Manning, A. D. Rosemond, R. L. Sinsabaugh, C. M. Swan, J. R. Webster, & L. H. Zeglin, 2017. Global synthesis of the temperature sensitivity of leaf litter breakdown in streams and rivers. Global Change Biology 23: 3064–3075, https://doi.org/10.1111/gcb.13609.

Forsyth, D. K., C. M. Riseng, K. E. Wehrly, L. A. Mason, J. Gaiot, T. Hollenhorst, C. M. Johnston, C. Wyrzykowski, G. Annis, C. Castiglione, K. Todd, M. Robertson, D. M. Infante, L.

Wang, J. E. McKenna, & G. Whelan, 2016. The Great Lakes hydrography dataset: Consistent, binational watersheds for the Laurentian Great Lakes basin. Journal of the American Water Resources Association 52: 1068–1088, https://doi.org/10.1111/1752-1688.12435.

Franken, R. J. M., R. G. Storey, & D. Dudley Williams, 2001. Biological, chemical and physical characteristics of downwelling and upwelling zones in the hyporheic zone of a north-temperate stream. Hydrobiologia 444: 183–195, https://doi.org/10.1023/A:1017598005228.

Godwin, C. M., & H. J. Carrick, 2008. Spatio-temporal variation of periphyton biomass and accumulation in a temperate spring-fed stream. Aquatic Ecology 42: 583–595, https://doi.org/10.1007/s10452-007-9133-z.

Graça, M. A. S., V. Ferreira, C. Canhoto, A. C. Encalada, F. Guerrero-Bolaño, K. M. Wantzen, & L. Boyero, 2015. A conceptual model of litter breakdown in low order streams. International Review of Hydrobiology 100: 1–12, https://doi.org/10.1002/iroh.201401757.

Griffiths, N. A., & S. D. Tiegs, 2016. Organic-matter decomposition along a temperature gradient in a forested headwater stream. Freshwater Science 35: 518–533, https://doi.org/10.1086/685657.

Harvey, J. W., & E. Bencala, 1993. The Effect of Streambed Topography on Surface-Subsurface Water Exchange in Mountain Catchments. 29: 89–98, https://doi.org/https://doi.org/10.1029/92WR01960.

Horner, R. R., E. B. Welch, M. R. Seeley, & J. M. Jacoby, 1990. Responses of periphyton to changes in current velocity, suspended sediment and phosphorus concentration. Freshwater Biology 24: 215–232, https://doi.org/10.1111/j.1365-2427.1990.tb00704.x.

Jowett, I. G., 1993. A method for objectively identifying pool, run, and riffle habitats from physical measurements. New Zealand Journal of Marine and Freshwater Research 27: 241–248, https://doi.org/10.1080/00288330.1993.9516563.

Kalbus, E., F. Reinstorf, & M. Schirmer, 2006. Measuring methods for groundwater - Surface water interactions: A review. Hydrology and Earth System Sciences 10: 873–887, https://doi.org/10.5194/hess-10-873-2006.

Krause, S., D. M. Hannah, & T. Blume, 2011. Ecohydrology Bearing - Invited Commentary

Transformation ecosystem change and ecohydrology: ushering in a new era for watershed management. Ecohydrology 4: 549–563, https://doi.org/10.1002/eco.199.

Kuznetsova, A., P. B. Brockhoff, & R. H. B. Christensen, 2017. lmerTest Package: Tests in Linear Mixed Effects Models. Journal of Statistical Software 82: 1–26, https://doi.org/10.18637/JSS.V082.I13.

Lavoie, I., S. Campeau, N. Zugic-Drakulic, J. G. Winter, & C. Fortin, 2014. Using diatoms to monitor stream biological integrity in Eastern Canada: An overview of 10 years of index development and ongoing challenges. Science of the Total Environment 475: 187–200, https://doi.org/10.1016/j.scitotenv.2013.04.092.

Lavoie, I., P. Hamilton, S. Campeau, M. Grenier, & P. J. Dillon, 2008. Guide d'identification des diatomées des rivières de l'Est du Canada. Presses de L'Université du Québec, Québec.

Legendre, P., & E. D. Gallagher, 2001. Ecologically meaningful transformations for ordination of species data. Oecologia 129: 271–280, https://doi.org/10.1007/s004420100716.

Lewandowski, J., S. Arnon, E. Banks, O. Batelaan, A. Betterle, T. Broecker, C. Coll, J. D. Drummond, J. G. Garcia, J. Galloway, J. Gomez-Velez, R. C. Grabowski, S. P. Herzog, R. Hinkelmann, A. Höhne, J. Hollender, M. A. Horn, A. Jaeger, S. Krause, A. L. Prats, C. Magliozzi, K. Meinikmann, B. B. Mojarrad, B. M. Mueller, I. Peralta-Maraver, A. L. Popp, M. Posselt, A. Putschew, M. Radke, M. Raza, J. Riml, A. Robertson, C. Rutere, J. L. Schaper, M. Schirmer, H. Schulz, M. Shanafield, T. Singh, A. S. Ward, P. Wolke, A. Wörman, & L. Wu, 2019. Is the hyporheic zone relevant beyond the scientific community? Water (Switzerland) 11:, https://doi.org/10.3390/w11112230.

Malard, F., & F. Hervant, 1999. Oxygen supply and the adaptations of animals in groundwater. Freshwater Biology 41: 1–30, https://doi.org/10.1046/j.1365-2427.1999.00379.x.

Martínez, A., A. Larrañaga, J. Pérez, E. Descals, & J. Pozo, 2014. Temperature affects leaf litter decomposition in low-order forest streams: field and microcosm approaches. Microbiology Ecology 87: 257–267, https://doi.org/10.1111/1574-6941.12221.

Mejia, F. H., C. V. Baxter, E. K. Berntsen, & A. K. Fremier, 2016. Linking groundwater – surface water exchange to food production and salmonid growth. Canadian Journal of Fisheries

and Aquatic Sciences 73: 1650–1660, https://doi.org/10.1139/cjfas-2015-0535.

Minshall, G. W., 1978. Autotrophy in stream ecosystems. BioScience 28: 767–771, https://doi.org/10.2307/1307250.

Mulholland, P. J., 1996. Role in nutrient cycling in streams In Stevenson, R. J., M. Bothwell, & R. Lowe (eds), Algal ecology: freshwater benthic ecosystems. Academic Press, San Diego, CA, USA: 609–639.

Oksanen, J., F. G. Blanchet, M. Friendly, R. Kindt, P. Legendre, D. McGlinn, P. R. Minchin, R. B. O'Hara, G. L. Simpson, P. Solymos, M. H. H. Stevens, E. Szoecs, & H. Wagner, 2020. vegan: community ecology package.

Ontario Geological Survey, 2010. Surficial geology of southern Ontario; Ontario Geological Survey, Miscellaneous Release Data 128 - Revised.

Passy, S. I., 2007. Diatom ecological guilds display distinct and predictable behavior along nutrient and disturbance gradients in running waters. Aquatic Botany 86: 171–178, https://doi.org/10.1016/j.aquabot.2006.09.018.

Petersen, R. C., & K. W. Cummins, 1974. Leaf processing in a woodland stream. Freshwater Biology 4: 343–368, https://doi.org/https://doi.org/10.1111/j.1365-2427.1974.tb00103.x.

Poisson, R., & A. G. Yates, 2022. Impaired cellulose decomposition in a headwater stream receiving subsurface agricultural drainage. Ecological Processes 11: 1–17, https://doi.org/10.1186/s13717-022-00406-9.

R Core Team, 2020. R: A language and environment for statistical computing. R Foundation for Statistical Computing, Vienna, Austria.

Renard, P., & D. Allard, 2013. Connectivity metrics for subsurface flow and transport. Advances in Water Resources Elsevier Ltd 51: 168–196, https://doi.org/10.1016/j.advwatres.2011.12.001.

Roy, J. W., B. Zaitlin, M. Hayashi, & S. B. Watson, 2011. Influence of groundwater spring discharge on small-scale spatial variation of an alpine stream ecosystem. 670: 661–670, https://doi.org/10.1002/eco.

Royer, T. V, & G. W. Minshall, 2003. Controls on leaf processing in streams from spatial-

scaling and hierarchical perspectives. Journal of the North American Benthological Society 22: 352–358, https://doi.org/https://doi.org/10.2307/1468266.

Sanchez, G., 2016. plsdepot: partial least squares data analysis methods. Version 0.1.17.

Stanford, J. A., J. V Ward, & B. K. Ellis, 1994. Ecology of the alluvial aquifers of the Flathead River, Montana In Gibert, J., D. L. Danielopol, & J. A. Stanford (eds), Groundwater Ecology. Academic Press, San Diego, USA: 367–390.

Steinman, A. D., G. A. Lamberti, & P. R. Leavitt, 2007. Biomass and pigments of benthic algae In Hauer, F. R., & G. Lamberti (eds), Methods in Stream Ecology. Academic Press, San Diego, CA, USA: 357–379, https://doi.org/https://doi.org/10.1016/B978-012332908-0.50024-3.

Štěrba, O., V. Uvíra, P. Mathur, & M. Rulík, 1992. Variations of the hyporheic zone through a riffle in the R. Morava, Czechoslovakia. Regulated Rivers: Research & Management 7: 31–43, https://doi.org/10.1002/rrr.3450070106.

Stevenson, R. J., 1997. Scale-dependent determinants and consequences of benthic algal heterogeneity. Journal of the North American Benthological Society 16: 248–262, https://doi.org/10.2307/1468255.

Stevenson, R., L. Novoveska, C. Riseng, & M. Wiley, 2009. Comparing responses of diatom species composition to natural and anthropogenic factors in streams of glaciated ecoregions. Nova Hedwigia 135: 1–13.

Storey, R. G., K. W. F. Howard, & D. D. Williams, 2003. Factors controlling riffle-scale hyporheic exchange flows and their seasonal changes in a gaining stream : A three-dimensional groundwater flow model. Water Resources Research 39: 1–17, https://doi.org/10.1029/2002WR001367.

Strommer, J. L., & L.A. Smock, 1989. Vertical distribution and abundance of invertebrates within the sandy substrate of a low-gradient headwater stream. Freshwater Biology 22: 263–274, https://doi.org/https://doi.org/10.1111/j.1365-2427.1989.tb01099.x.

Thibodeaux, L., & J. Boyle, 1987. Bedform-generated convective transport in bottom sediment. Nature 325: 341–343, https://doi.org/doi-org/10.1038/325341a0.

Tiegs, S. D., P. O. Akinwole, & M. O. Gessner, 2009. Litter decomposition across multiple spatial scales in stream networks. Oecologia 161: 343–351, https://doi.org/10.1007/s00442-009-1386-x.

Tiegs, S. D., J. E. Clapcott, N. A. Griffiths, & A. J. Boulton, 2013. A standardized cotton-strip assay for measuring organic-matter decomposition in streams. Ecological Indicators 32: 131–139, https://doi.org/10.1016/j.ecolind.2013.03.013.

Tiegs, S. D., D. Costello, M. Isken, G. Woodward, P. McIntyre, M. O. Gessner, E. Chauvet, N. A. Griffiths, A. Flecker, V. Acuña, & R. Albariño, 2019. Global patterns and drivers of ecosystem functioning in rivers and riparian zones. Science Advances 5: 1–8, https://doi.org/10.1126/sciadv.aav0486.

Van Dam, H., A. Mertens, & J. Sinkeldam, 1994. A coded checklist and ecological indicator values of freshwater diatoms from The Netherlands. Netherlands Journal of Aquatic Ecology 28: 117–133, https://doi.org/10.1007/BF02334251.

Vissers, M. A., J. W. Roy, A. G. Yates, K. Robinson, S. Rakhimbekova, & C. E. Robinson, 2023. Spatio-temporal variability of porewater phosphorus concentrations in streambed sediments of an agricultural stream. Journal of Hydrology Elsevier B.V. 617: 129133, https://doi.org/10.1016/j.jhydrol.2023.129133.

Webb, J. R., N. J. T. Pearce, K. J. Painter, & A. G. Yates, 2019. Hierarchical variation in cellulose decomposition in least-disturbed reference streams: a multi-season study using the cotton strip assay. Landscape Ecology 34: 2353–2369, https://doi.org/10.1007/s10980-019-00893-w.

Wold, S., M. Sjöström, & L. Eriksson, 2001. PLS-regression: A basic tool of chemometrics. Chemometrics and Intelligent Laboratory Systems 58: 109–130, https://doi.org/10.1016/S0169-7439(01)00155-1.

Wyatt, K. H., F. R. Hauer, & G. F. Pessoney, 2008. Benthic algal response to hyporheic-surface water exchange in an alluvial river. Hydrobiologia 607: 151–161, https://doi.org/10.1007/s10750-008-9385-1.

Statements and Declarations

Funding: CER and AGY were awarded a Natural Sciences and Engineering Research Council of Canada Strategic Project Grant (STPG 506523) to CER and AGY. LKB received an Ontario Graduate Scholarship (2019) and NSERC Postgraduate Scholarship (2020).

Competing Interests: The authors have no relevant financial or non-financial interests to disclose.

Data Availability: The datasets generated during and/or analysed during the current study are available from the corresponding author on reasonable request.

Author Contributions: Conceptualization: LKB, AGY, CER, JWR; Methodology: LKB, AGY, CER, JWR; Formal analysis and investigation: LKB, AGY; Technical Support: LKB; Writing - original draft preparation: LKB, AGY; Writing - review and editing: IL, CER, JWR, and AGY; Funding acquisition: CER, AGY; Resources: IL, CER, AGY; Supervision: AGY

Supplemental Information

1. Radon-222 mass balance model

Groundwater discharge along each stream reach was estimated by applying a steady state ^{222}Rn mass balance model in which gas exchange and radioactive decay of ^{222}Rn in the stream was taken into account. Using this model, groundwater inflows (q_{gw}, m^3/m/d) along the stream reaches were estimated via (Atkinson et al., 2015; Cook, 2013; Mullinger et al., 2007):

$$q_{gw} = \frac{Q_s \frac{(C_{out} - C_{in})}{L} - kdwC_s + \lambda \mathrm{d}wC_s}{(C_{gw} - C_s)}$$

where C_{in} and C_{out} are the ^{222}Rn activities measured at the downstream and upstream sampling for the reach (Bq/m^3), C_s is the average ^{222}Rn activity in the stream reach considering the upstream and downstream activities (Bq/m^3), C_{gw} is a representative ^{222}Rn activity in the groundwater, d and w are the average stream depth and width, respectively (m), Q_s is the average stream discharge (m^3/day), λ is the radioactive decay rate (0.181 day^{-1}) and k is the reaeration coefficient (day^{-1}). ^{222}Rn loss due to evaporation was not included as it is not expected to considerably affect the ^{222}Rn concentrations in the stream (Atkinson et al., 2015). C_{gw} was based on sampling of six shallow groundwater wells located within 20 m of Kintore Creek (6700 ± 1400 Bq/m^3).

The reaeration coefficient (k) defines the rate of degassing of ^{222}Rn across the air-water interface and is related to stream turbulence. Following Atkinson et al. (2015), the following empirical relationship which is a modification of the gas transfer model of O'connor and Dobbins (1958) was used to calculate k:

$$k = 9.301\ x\ 10^{-3} \left(\frac{v^{0.5}}{d^{1.5}}\right)$$

where v is the average river velocity in the stream reach. Other empirical relationships were explored to estimate k including that based on the gas transfer model of Negulescu and Rojanski (1969), but the calculated groundwater inflow patterns were consistent regardless of which relationship was adopted.

Table S.1 Additional input information for ^{222}Rn steady state mass balance model for three reaches in Kintore Creek, Ontario, Canada receiving high (HG), moderate (MG) and low (LG) inputs of groundwater.

	HG	MG	LG
^{222}Rn Above Reach (Bq m^{-3})	1183	294	679
^{222}Rn Below Reach (Bq m^{-3})	1121	679	762
Average stream flow (m^3/s)	0.041	0.010	0.015
Distance between sampling points (m)	174	191	210
Average stream depth (m)	0.15	0.11	0.12
Average stream width (m)	2.00	0.89	0.87
Average stream velocity (m/s)	0.14	0.10	0.15

References

Atkinson, A.P. et al., 2015. A multi-tracer approach to quantifying groundwater inflows to an upland river; assessing the influence of variable groundwater chemistry. Hydrological Processes, 29(1): 1-12.

Cook, P.G., 2013. Estimating groundwater discharge to rivers from river chemistry surveys. Hydrological Processes, 27(25): 3694-3707.

Mullinger, N.J., Binley, A.M., Pates, J.M., Crook, N.P., 2007. Radon in Chalk streams: Spatial and temporal variation of groundwater sources in the Pang and Lambourn catchments, UK. Journal of Hydrology, 339(3-4): 172-182.

O'Connor, D., Dobbins, W.E., 1958. Mechanism of Reaeration in Natural Streams. Transactions of the American Society of Civil Engineers, 123: 641-666.

Negulescu, M., Rojanski, V., 1969. Recent research to determine reaeration coefficient. Water Research, 3(3): 189-202.